SPIE '98,

Micromachined High Q inductors For High Frequency Applications

Jae Y. Park and Mark G. Allen
School of Electrical and Computer Engineering
Georgia Institute of Electrical and Computer Engineering
Atlanta, GA 30332-0269

ABSTRACT

To meet requirements in mobile communication and microwave integrated circuits, miniaturization of the inductive components that many of these systems require is of key importance. At present, active circuitry is used which simulates inductor performance and which has high Q-factor and inductance; however, such circuitry has higher power consumption and higher potential for noise injection than passive inductive components. An alternate approach is to fabricate integrated inductors, in which lithographic techniques are used to pattern an inductor directly on a substrate or a chip. However, integrated inductors can suffer from low Q-factor and high parasitic effects due to substrate proximity. To expand the applications of integrated inductors, these characteristics must be improved.

High Q integrated spiral inductors are investigated using polymer/metal multilayer processing techniques and surface micromachining techniques. These inductors have spiral geometry with an air core and a large air gap (40μm height) between the coils and the substrate (to reduce substrate capacitance), and thick, highly conductive electroplated copper conductor lines (to increase the quality factor). Various inductor geometries are investigated by designing and fabricating several inductors with differing core areas and numbers of turns. The fabricated inductors have a Q-factor of 40~75 at 300~700 MHz and an inductance at these frequencies between 30~70nH.

Keywords: high Q inductors, integrated, low temperature processes, surface micromachining, polymer/metal multilayer processing, electroplating

1. INTRODUCTION

There are a large number of discrete passives and relatively fewer integrated circuits (ICs) required in many consumer electronic products such as VCRs, pagers, cellular phones, GPS receivers, and camcorders or other RF or mixed-signal systems. The impact of the large number of discrete passives on system cost, size, weight, and reliability is substantial. An approach to addressing these issues is integrating these passive components directly into a multichip module (MCM) or other packaging substrate [1-2]. Using this approach, the size of the board can be reduced (especially if chips can be placed above embedded passive components) and the parasitics associated with the passive components may also be reduced due to the elimination of leads and the shorter connections between passive components and other IC chips.

Due to these limitations, two-dimensional structures, typically spiral coils supported on substrates, have been fabricated. For example, a thin film LC filter has been fabricated by RF sputtering and ion-milling techniques [3]. A passives filter with a multilayer thin-film air core inductor for the 850 MHz band was demonstrated in [4]. A large suspended inductor on silicon for RF amplifier applications was fabricated in [5]; the deleterious effects of the silicon substrate were reduced by selectively etching out the silicon under the inductor. Transistor-integrated suspended spiral inductors formed from the metallization used in GaAs technologies have been produced; using air-bridge technologies, these devices have a typical air gap of 3 μm between the conductor lines which form the inductor and the substrates [6]. Solenoid-type inductors have also been produced using a combination of electroplating and micromachining techniques that are suspended approximately 20 μm above the substrate [7]; such devices have reported Q-factors ranging from 30-60.

J.Y.P. (correspondence): E-mail: jae.park@ece.gatech.edu; www: http://prsim.gatech.edu/~jp91; Telephone: 404-894-8807; Fax: 404-894-5028
M.G.A.: mallen@ece.gatech.edu; Telephone: 404-894-9419; Fax: 404-894-5028

Another issue in the fabrication of integrated passive components is temperature compatibility. Much research has been done to realize integrated passive components based on MCM-C (ceramic) and MCM-D (deposited) technology [8-10]. In much of this research, it is usually necessary to undergo high temperature fabrication steps such as firing of conductive pastes or ceramics. However, in many cost-driven applications that require the use of organic laminate substrates, the use of low temperature fabrication steps is necessary in the realization of these passive components. In this research, suspended air core inductors and a low pass filter are designed, fabricated, and characterized using low temperature fabrication processes, MCM-L, and MCM-D technology, to test the feasibility of integration of passives for wireless applications.

2. DESIGN AND MODELING

For high frequency applications, it is most appropriate to consider air-core inductor devices, since the high frequency behavior of many magnetic core materials is relatively poor. The characteristics of an integrated inductor with a non-magnetic core can be determined solely by the coil geometry and location. In addition to accurate determination of the inductance of air-core inductors, it is also important at high frequency to assess parasitic effects such as stray capacitance and conductor skin effect in order to understand the effective operation of the device. Much research has been done to analyze the stray capacitance of an integrated inductor in high frequency applications [11-13]. The stray capacitance of the inductor determines the self resonant frequency (SRF) and the Q-factor. Therefore, the stray capacitance should be kept low. Various aspects of the inductor geometry, such as the cross-sectional area of the conductor line, the line spacing, and the core size, must be considered such that the inductor has the desired performance after fabrication.

The resistivity of the conductor should be low to obtain a high Q-factor at very high frequencies. Since high frequency current flows mostly along the surface area of a conductor, the skin effect causes the winding resistance to increase as the frequency is increased. The skin depth of the conductor is given by:

$$\delta = \frac{1}{\sqrt{f\pi\mu\sigma}}, (m) \qquad (1)$$

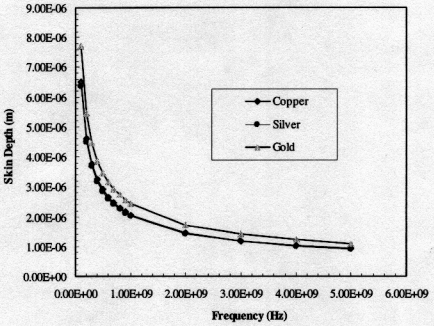

Figure 1. Skin depth of commonly used conductor materials such as silver, copper, and gold as a function of frequency

where f represents frequency, μ permeability, and σ conductivity. Figure 1 shows the skin depth of commonly used conductor materials such as silver, copper, and gold calculated using the skin depth equation. Literature resistivity values of silver, copper, and gold of 1.59×10^{-8} ohm-m, 1.67×10^{-8} ohm-m, and 2.35×10^{-8} ohm-m respectively were used to calculate the skin depth. Thicknesses of conductor lines much in excess of several skin depths at the frequency of interest will not greatly reduce the conductor resistance or increase the inductor Q-factor.

A spiral inductor design is considered for the realization of a high-Q integrated inductor due to its simplicity of fabrication as well as its large achievable core cross-sectional area. Yamaguchi *et al.* [14] have reported the stray capacitance of various parts of thin film inductors employing meander and spiral-type coils. It was reported that for inductors in direct contact with the substrate that the capacitance between conductor lines was relatively small compared with that produced by the substrate-to-conductor coupling.

Figure 2 shows a schematic drawing of an integrated spiral inductor with a large air gap between the conductor lines and the substrate. The air gap is maintained by plated copper metal supports that allow the air gap to be large compared with traditional air bridge approaches, thus reducing the stray capacitance from the substrate. Thick (e.g., electrodeposited) conductor lines (i.e., several skin depths) are also necessary to increase the cross-sectional area of the conductor and to reduce the conductor resistance. Electroplated copper is useful to achieve thick conductor lines for integrated inductors and interconnections.

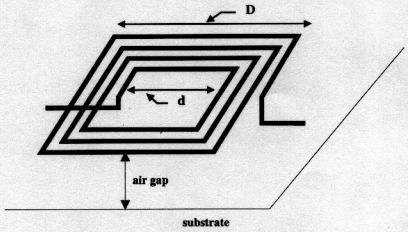

Figure 2. A schematic drawing of an integrated spiral inductor with a large air gap

At frequencies on the order of several hundred MHz and above, it is usually necessary to use air (or dielectric) cores in inductors due to the magnetic losses associated with many magnetic core materials at these frequencies. Thus, the quality factor of the integrated inductor is strongly dependent upon the coil windings and stray capacitance between windings and substrate. Air core solenoid type inductors may be easily affected by nearby metallic surfaces due to their high leakage inductance. As shown in Equation (2), a square spiral inductor may be defined by the 5 independent geometric variables in free space [15].

$$L_s = F(D+d, D-d, N, s, t) \tag{2}$$

where D and d are the outermost and innermost dimensions, respectively, as shown in Figure 2; and N, s, and t are the number of turns, line spacing and metal thickness of the given square spiral inductor. Bryan found an empirical equation to calculate the inductance of a square spiral-type inductor at high frequency based on these variables [16]:

$$L_s = kaN^r \ln(8a/c) \tag{3}$$

where:

$$a = \frac{D+d}{2}, c = \frac{D-d}{2} \tag{4}$$

The variable k has units of inductance per unit length, and is dependant on the conductor material as well as on the geometric variables s and t; it is also dependent on the thickness of the substrate on which the inductors are formed (if a ground plane exists on the other side of the substrate). This semi-empirical equation separates out an explicit geometric dependence on number of turns and conductor x-y dimensions from an implicit geometric dependence on conductor spacing and thickness (which is lumped into the variable k). Thus, for inductors of similar conductor spacing and thickness, but varying size and number of turns, the variable k is expected to be a constant if equation (3) is obeyed.

The self resonant frequency (SRF) of the integrated inductor is defined as follows:

$$f_0 = \frac{1}{2\pi\sqrt{LC}}\left(1 - \frac{1}{Q_0^2}\right) \tag{5}$$

where Q_0 is the unloaded Q of the inductor not including parasitic capacitance due to bonding pads and interconnect. The unloaded Q is found by taking the ratio of the imaginary part of the inductor impedance to the real part of the inductor impedance (neglecting bonding pads and interconnect):

$$Q_0 = \frac{\omega L}{R_L(f)} \tag{6}$$

A high quality factor means that the inductor has the desirable properties of low dissipation and favorable frequency characteristics when utilized in filter circuits. A high Q-factor can be achieved by reducing the series resistance, (i.e., using highly conductive material, short conductor lines, and conductors with thickness equal to several skin depths), and reducing the stray capacitance between windings and the substrate, especially if the substrate is lossy. The substrate stray capacitance can be reduced by introducing a large air gap between the substrate and the spiral coils. Such large air gaps can be achieved using a surface micromachining technique and a polyimide, photoresist, or other organic sacrificial layer.

3. FABRICATION OF HIGH Q MICROINDUCTORS

The fabricated high Q spiral-type inductors are suspended from the substrate using thick electroplated copper metal posts. Figure 3 shows the fabrication sequence of the integrated high Q spiral-type inductor. A Ti/Cu/Ti seed layer was deposited on the cleaned glass substrate and polyimide (Dupont PI-2611) was then coated on top of the deposited seed layer to build electroplating molds for posts, test pads, and grounds. Two coats were applied to obtain 20 μm thick polyimide molds. Each coat was cast at 600 rpm for 20 seconds, 3500 rpm for 4 seconds, and soft-baked at 120 °C in a convection oven for 10 minutes prior to the application of next coat. After spin-casting all coats, the polyimide was hard-cured at 220 °C for 0.5 hours and 350 °C for 1 hour in nitrogen. The polyimide molds were formed using plasma O_2 etch and an aluminum hard mask. The electroplating molds were then filled with copper using standard electroplating techniques. Two coats of polyimide on top of the plated copper metal were spun and hard-cured. Electroplating molds were formed for upper posts to support conductor lines and via connections between selected posts and spiral-type conductor lines. The electroplating forms were then filled with copper using standard electroplating techniques. A seed layer (Ti/Cu/Ti) was then deposited and 20 μm thick photoresist was coated on the seed layer and patterned to form additional electroplating molds. The electroplating molds were again filled with copper using standard electroplating techniques. The photoresist molds were then removed and the seed layer wet-etched. Plasma etching using 80 % O_2 and 20 % CHF_3, was used to remove all polyimide on top of the substrate. The addition of the CHF_3 gas also facilitated the removal of the polyimide under the metal conductor lines. After removing all polyimide, the bottom seed layer was wet-etched.

Figure 4 shows a scanning electron micrograph (SEM) of the high Q inductor suspended over the substrate using plated posts. Figures 5 and 6 show scanning electron micrographs (SEM) of large suspended spiral conductor lines, plated posts, vias, and signal connection under the conductor lines. Figure 7 shows a close up view of large-gap suspended (40 μm) spiral conductor lines and plated posts of the high Q inductor.

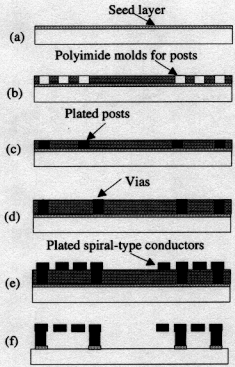

Figure 3. Fabrication sequences of the high Q inductor: (a) seed layer deposition; (b) formation of polyimide molds for posts; (c) plating of posts (copper) (d) via formation; (e) formation of spiral type conductor lines using electroplating techniques; (f) removal of polyimide using plasma etcher and seed layer using wet-etching solutions.

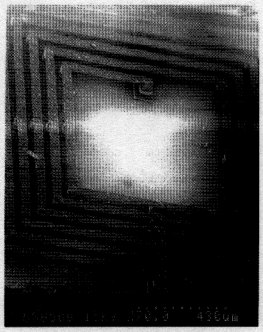

Figure 4. Scanning electron micrograph of suspended integrated high Q inductor.

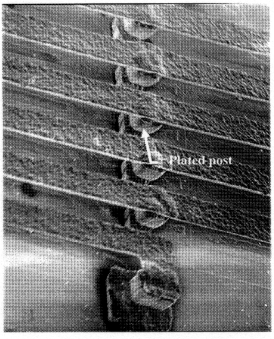

Figure 5. Scanning electron micrograph of suspended plated spiral conductor lines and plated thick posts of the integrated high Q inductor.

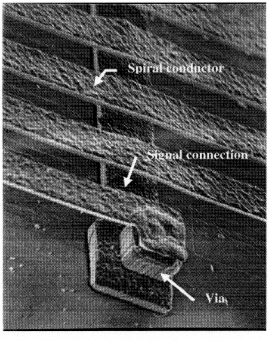

Figure 6. Scanning electron micrograph of large suspended plated spiral conductor lines and signal connection through plated via.

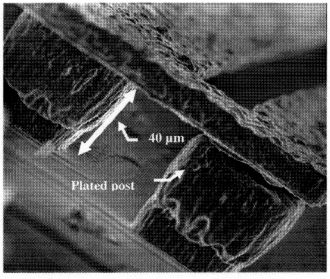

Figure 7. Scanning electron micrograph of electroplated via posts (40 μm height) to support the spiral conductor lines in the air.

4. EXPERIMENTAL RESULTS AND DISCUSSIONS

The fabricated air core spiral-type inductors have been measured using an HP 8510C Network Analyzer terminated with 50 ohms and CASCADE MICROTECH ground-signal-ground high frequency coplanar probes with 150 μm pitch size. The measured two-port S-parameters were transformed into one-port S-parameters by terminating one port with ground at a HP Microwave and RF Design System (MDS). A reflection coefficient, S_{11} of the transformed one-port S parameters was translated into an input impedance, Z_{11} for evaluating inductance and quality factor of fabricated inductors using an HP Microwave and RF Design System (MDS). The unloaded Q-factor was determined by dividing the imaginary part by the real part (dissipated energy) of the input impedance, Z_{11}. The inductance can be calculated using a simplified equivalent circuit in which the inductor is connected in series with a coil resistance and in parallel with a parasitic capacitance. The inductance was computed by dividing the imaginary part (inductive stored energy) by the frequency, ω, since the effect of the parasitic capacitance in these structures and at these frequencies was small (with the exception of the largest inductor).

Table 1 shows a list of the different geometries of the designed air core spiral-type inductors. These inductors have 40 μm wide and 15 μm thick electroplated copper conductor lines, and the spacing between the windings is 40 μm. All inductors are suspended over the substrate by 40 μm air gaps. We were observed process variation 10~20 % in this geometry due to the thick photoresist used.

Table 1. Designed parameters of fabricated spiral-type inductors with air core

Type	Dimension of fabricated inductors (mm)	Width, thickness, and spacing of conductor lines (μm)	Core area (mm)	Number of turns
A	1.5 x 1.5	40 x 15 x 40	0.46 x 0.46	7.5
B	1.9 x 1.9	40 x 15 x 40	1.1 x 1.1	5.5
C	2.2 x 2.2	40 x 15 x 40	1.1 x 1.1	7.5

Table 2. Comparison of measured and calculated inductance of the fabricated spiral-type air core inductors

Type	Measured inductance (nH)	Calculated inductance (nH)
A	34	34.24
B	40	40.18
C	70	69.61

The measured dc resistance of the fabricated inductors varies from 0.9 to 1.1 ohms, depending on the length of conductor lines; these values are well matched with calculated values based on conductor line geometry and the low frequency resistivity of electroplated copper.

Figures 8, 9, and 10 show inductive part of input impedance and quality factor as a function of frequency of the air core spiral inductors. As both the number of turns and core area are increased, the inductance is increased as predicted. However, as frequency is increased, the inductors with large number of turns produce lower quality factor and self resonant frequency, since the longer conductor lines produce higher series resistance and stray capacitance. At high frequencies, short conductor lines and large core area are required to have high quality factor and self resonant frequency (SRF).

Table 2 shows a comparison of measured and calculated inductance of the fabricated suspended air core spiral inductors. The calculated inductance was evaluated using Equations (3) and (4), in which the variable k was used as a variable fitting coefficient, and the best-fit value of k, 0.488 nH/mm, was used in the prediction of all of the inductor values. Even though only one fitting coefficient was used, good agreement between equation (3) and the experimental data was observed, indicating that equation (3) captures the dependence of the inductance on inductor size and number of turns very well.

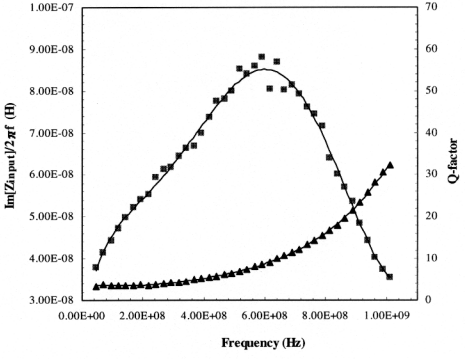

Figure 8. Quality factor and inductive part of input impedance of the fabricated A-type air core spiral inductors suspended from the substrate.

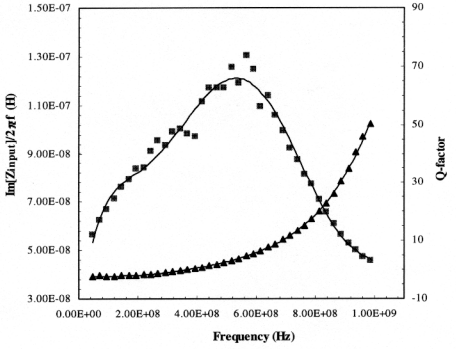

Figure 9. Quality factor and inductive part of input impedance of the fabricated B-type air core spiral inductors suspended from the substrate.

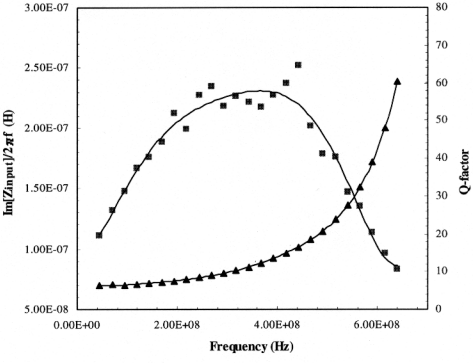

Figure 10. Quality factor and inductive part of input impedance of the fabricated C-type air core spiral inductors suspended from the substrate.

As shown in Table 1, A, B, and C type inductors have the same conductor geometries, while each having a different number of turns and different core area. At constant overall dimension, as the number of turns is increased, the core area is decreased. As the number of turns is decreased, the inductance is decreased, while the Q-factor is increased because of the reduced series resistance and stray capacitance. As the number of turns is increased, the inductance is increased and the Q-factor is decreased because of the increased resistance and stray capacitance as predicted. In the comparison of these fabricated inductors, the B-type inductor has the highest Q-factor, approximately 75 at 570 MHz. Although the C-type inductor has the highest inductance, it has the lowest Q-factor, approximately 58at 280 MHz. Obviously, increasing the number of turns increases the inductance. However, this increases the resistance and the stray capacitance of the inductor, which lowers the self resonant frequency and Q-factor.

5. CONCLUSIONS

Large suspended integrated spiral microinductors with air core for high frequency applications have been proposed and fabricated using low temperature MCM-D/L technology combined with surface micromachining techniques. A 40 μm air gap is introduced between the spiral-type conductor lines and the substrate to achieve high Q-factor by reducing the stray capacitance of the lossy substrate which is dominant in the total stray capacitance. The air gap was realized by supporting the spiral-type conductor lines using plated copper posts at the edges and at the center of the conductor lines.

Fabricated inductors with various geometries have been compared. As the number of turns is increased, the inductance, resistance, and stray capacitance are also increased. The increased resistance and stray capacitance reduce the Q-factor and the self resonant frequency. These inductors with high inductance, Q-factor, and low dc resistance are useful for communications, signal processing, MMIC circuitry, and analog circuitry applications.

ACKNOWLEDGEMENT

This research was supported in part by the National Science Foundation through the Georgia Tech /NSF Engineering Research Center in Electronic Packaging (contract EEC- 9402723). Fabrication was carried out at the Microelectronics Research Center of Georgia Tech. The authors also acknowledge the Microsensor and Microactuator (MSMA) Group and Microelectronics Research Center staff for their help with processing questions. Valuable technical discussions and assistance of Dr. Young Jun Kim of Samsung Electronics in Korea is also greatly appreciated.

REFERENCES

[1] J. Park and M. Allen, "Low temperature fabrication and characterization of integrated packaging-compatible, ferrite-core magnetic devices", *IEEE 12th Applied Power Electronicc Conference*, pp. 361-367, 1997

[2] J. Park and M. Allen, "Packaging-compatible microinductors and microtransformers with screen-printed soft ferrite using low temperature processes", *IEEE 7th Joint MMM-Intermag Conference*, California, 1998

[3] M. Yamaguchi, K. Ishihara, and K. Arai, "Application of thin-film inductors to LC filters", *IEEE Transactions on Magnetics*, vol. 29, no. 6, pp. 3222-3225, 1993

[4] V. Sadhir, I. Bahl, and D. Willems, "CAD compatible accurate models of microwave passive lumped elements for MMIC applications", *International Journal of Microwave and Millimeter-Wave Computer-Aided Engineering*, vol. 4, no. 2, pp. 148~162, 1994

[5] J.Y. C. Chang, A. A. Abidi, and M. Gaitan, "Large suspended inductors on silicon and their use in a 2 μm CMOS RF amplifier", *IEEE Electron Devices Letters*, vol. 14, no. 5, May 1993

[6] M. E. Goldfarb and V. K. Tripathi, "The effect of air bridge height on the propagation characteristics of the microstrip", *IEEE Microwave Guided Wave Letter*, vol. 1, pp. 273-274, Oct. 1991

[7] Y. J. Kim and M. G. Allen, "Solenoid type high frequency inductor", *IEEE Transactions on Component, Packaging, and Manufacturing Technology (Part-C)*, (to be published in 1998)

[8] R. Frye, K. Tai, M. Lau, and A. Lin, "Low-cost silicon-on-silicon MCMs with integrated passive components", *Proceedings of the 1992 International Electronics Packaging Conference*, vol. 1, pp. 343, 1992

[9] R. Brown, A. Shapiro, and P. Polinski, "The integration of passive components into MCMs using advanced low temperature co-fired ceramics", *International Journal of Microcircuits and packaging*, vol. 16, no. 4, pp. 328-338, 1993

[10] P. Mccaffrey, "Integrated passive components for silicon hybrid multichip modules", *Proceedings of the International Electronics Packaging Conference*, pp. 411-420, 1990

[11] A. Massarini, M. Kazimierczuk, and G. Grandi, "Lumped parameter models for single- and multiple-layer inductors", *27th Annual IEEE Power Electronics Specialists Conference*, vol.1, pp.295-301, 1996

[12] G. Grandi, M. Kazimierczuk, A. Massarini, and U. Reggiani, "Stray capacitances of single-layer air-core inductors for high-frequency applications", IAS'96. *IEEE Industry Applications Conference*, pp.1384-8 vol.3, 1996

[13] B. Breen, "Multi-layer inductor for high frequency applications", *41st Electronic Components and Technology Conference*, pp.551-4, 1991

[14] M. Yamaguchi, M. Matsumoto, H. Ohzeki and K. I. Arai, "Analysis of the inductance and the stray capacitance of the dry-etched micro inductors", *IEEE Trans. Magnetics*, Vol. 27, No 6, 5274-5276, Nov. 1991

[15] Ping Li, "A new closed form formula for inductance calculation in microstrip line spiral inductor design", *Electrical Performance of Electronic Packaging*, pp.58-60, 1996

[16] H. Bryan, "Printed inductors and capacitors", Tele-Tech & Electronic Industries, PP. 68, 1955